A Simple Route for Low-Temperature Synthesis of Mesoporous and Nanocrystalline Anatase Thin Films

Florence Bosc,*,† André Ayral,† Pierre-Antoine Albouy,‡ and Christian Guizard†

Institut Européen des Membranes, UMR CNRS 5635, CC047, Université Montpellier II, F-34095 Montpellier Cedex 5, France, and Laboratoire de Physique des Solides, UMR CNRS 8502, Bâtiment 510, Université de Paris-Sud, F-91405 Orsay, France

Received January 28, 2003. Revised Manuscript Received March 20, 2003

A simple sol−gel route has been developed for the preparation of mesoporous and nanocrystalline anatase thin layers. An anatase hydrosol was first synthesized at room temperature from acidic hydrolysis of titanium isopropoxide. The optimization of the synthesis parameters, including titanium concentration, HCl/Ti and H_2O/Ti ratios, temperature, and aging time, enabled us to produce a clear sol with a very low HCl/Ti ratio (equal to 1). As a function of the further thermal treatment conditions, it was then possible to control the size of the anatase crystallites (from 5 to >10 nm) and the O/Ti stoichiometry (from 1.9 to 2.0). Ordered mesoporosity was obtained by using a triblock copolymer as the templating agent. Preliminary experiments evidenced the photocatalytic activity of the prepared layers.

Introduction

Titania is a semiconducting oxide that has been extensively investigated because of its photoactivity under near-UV light with potential applications such as photovoltaics or photocatalysis. Its application to the purification of water or air has been particularly considered.[1,2] The photoactivity of TiO_2 is strongly dependent on its crystalline structure, on the crystallite size, and on the synthesis method used.[3] The anatase crystalline form appears to be the most active.[4,5] The optimal crystallite size is in the range 8−10 nm. Smaller crystallite sizes favor surface recombination, whereas larger crystallites exhibit lower efficiencies.[6]

The preparation of nanocrystalline anatase thin films is of great importance for existing or potential technological applications such as photovoltaic cells, self-cleaning windows, electrochemical devices and sensors, coupling membrane separations, and photocatalytic reactions. A key point for some applications is the ability to form anatase layers at low temperature on substrates exhibiting a low thermal stability such as plastics. Moreover, the accessibility of the chemical species to the titania surface is strongly conditioned by the porous characteristics of the layer: the pore volume, the pore size, the connectivity, and the tortuosity of porous network. An attractive method for tailoring the porosity consists of using the templating effect of mesophases produced by the self-assembly of amphiphilic molecules.[7] Several papers report recent studies on the sol−gel synthesis of mesoporous titania layers using cationic surfactants[8−10] or diblock[11] or triblock copolymers[12−16] as structuring agents and titanium chloride,[11−13,15] titanium alkoxide,[9,10,14,16] or a titanium derivative of triethanolamine[8] as the titania precursor. The as-prepared titania layers are mainly amorphous, and thermal nucleation and crystal growth of anatase usually occur for temperatures higher than 350 °C and are often associated with the disappearance of the ordered mesoporosity.

This study deals with the development of a simple sol−gel route for the synthesis at low temperature of mesoporous and nanocrystalline anatase thin films exhibiting attractive photocatalytic properties. The synthesis conditions are discussed first. The thermal evolution of the supported layers and of the corresponding powders is then detailed. Finally, preliminary

* To whom correspondence should be addressed. E-mail: Florence.Bosc@iemm.univ-montp2.fr.
† Université Montpellier II.
‡ Université de Paris-Sud.

(1) Fujishima, A.; Hashimoto, K.; Watanabe, T. *TiO_2 Photocatalysis—Fundamentals and Applications*; BKC, Inc.: Tokyo, 2001.
(2) Pichat, P.; Disdier, J.; Hoang-Van, C.; Mas, D.; Goutailler, G.; Gaysse, C.; *Catal. Today* **2000**, *63*, 363.
(3) Gao, L.; Zhang, Q. *Scr. Mater.* **2001**, *44*, 1195.
(4) Hsien, Y. H.; Chang, C. F.; Chen, Y. H.; Cheng, S. *Appl. Catal.* **2001**, *31*, 241.
(5) Schindler, K. M.; Kunst, M. *J. Phys. Chem.* **1990**, *94*, 8222.
(6) Zhang, Z.; Wang, C.-C.; Zakaria, R.; Ying, J. Y. *J. Phys. Chem. B* **1998**, *102*, 10871.
(7) Klotz, M.; Ayral, A.; Guizard, C.; Cot, L. *Bull. Korean Chem. Soc.* **1999**, *20*, 879.
(8) Cabrera, S.; El Haskouri, J.; Beltran-Porter, A.; Marcos, M. D.; Amoros, P. *Solid State Sci.* **2000**, *2*, 513.
(9) Yusuf, M. M.; Imai, H.; Hirashima, H. *J. Non-Cryst. Solids* **2001**, *285*, 90.
(10) Yusuf, M. M.; Imai, H.; Hirashima, H. *J. Sol−Gel Sci. Technol.* **2002**, *25*, 65.
(11) Hwang, Y. K.; Lee, K.C.; Kwon, Y.U. *Chem. Commun.* **2001**, 1738.
(12) Kavan, L.; Rathousky, J.; Grätzel, M.; Shklover, V.; Zukal, A. *J. Phys. Chem. B* **2000**, *104*, 12012.
(13) Grosso, D.; Soler-Illia, G. J. A. A.; Babonneau, F.; Sanchez, C.; Albouy, P. A.; Brunet-Bruneau, A.; Balkenende, A. R. *Adv. Mater.* **2001**, *13*, 1085.
(14) Yun, B. S.; Miyazawa, K.; Zhou, H.; Honma, I.; Kuwabara, M. *Adv. Mater.* **2001**, *13*, 1377.
(15) Alberius, P. C. A.; Frindell, K. L.; Hayward, R. C.; Kramer, E. J.; Stucky, G. D.; Chmelka, B. F. *Chem. Mater.* **2002**, *14*, 3284.
(16) Crepaldi, E. L.; Soler-Illia, G. J. d. A. A.; Grosso, D.; Sanchez, C. *New J. Chem.* **2003**, *27*, 9.

10.1021/cm031025a CCC: $25.00
Published on Web 05/16/2003

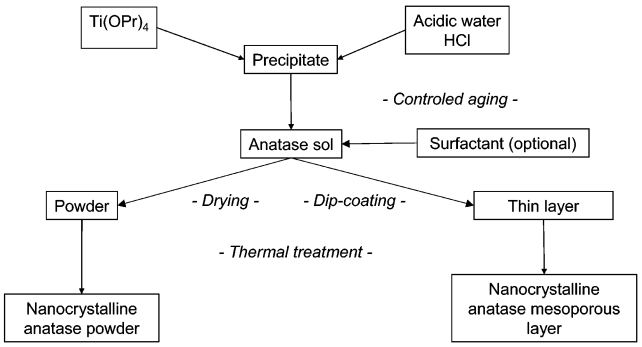

Figure 1. Flowchart of the overall procedure for the preparation of the thin films and equivalent powders.

results on the photocatalytic properties of the prepared layers are presented.

Experimental Section

Preparation Methods. The flowchart of the overall synthesis procedure is shown in Figure 1. The chosen titania precursor was a common reagent, titanium isopropoxide. This precursor is significantly less reactive than titanium chloride, which has typically been used to prepare ordered mesoporous titania and which requires restricting anhydrous conditions during the first stages of the synthesis. The titanium isopropoxide was hydrolyzed under vigorous stirring by the addition of an aqueous solution of hydrochloric acid. This first stage of the synthesis was optimized by varying the following parameters: the titanium concentration in the sol, $0.5 < [Ti] < 10.0$ mol L^{-1}; the HCl/Ti ratio, $0.5 < a < 2.0$; the H_2O/Ti hydrolysis ratio, $6 < h < 30$; and the temperature, 20 °C $< \theta <$ 35 °C. After aging times depending of the synthesis parameters, the peptization of the initial precipitate occurs, giving rise to a clear sol. During the third stage, the precipitation of a new white solid occurs. Our strategy of synthesis optimization was to determine the lowest HCl/Ti ratio required to obtain a clear aqueous sol so that the chloride content in the formed solid would be minimized. Using this criterion, the following values were selected for the synthesis parameters: [Ti] = 1.0 mol L^{-1}, $a = 1.0$, $h = 20.0$, and $\theta = 30$ °C.

To generate ordered mesoporosity by the templating effect, the sols were aged for 3 h before a structuring agent was added under stirring. The selected surfactant was the triblock copolymer poly(ethylene oxide)−poly(propylene oxide)−poly(ethylene oxide), $EO_{20}PO_{70}EO_{20}$, labeled P_{123} (provided by BASF). This large amphiphilic molecule exhibits several advantages, including the existence of a hexagonal columnar mesophase in its binary diagram with water[17] and the ability to accommodate large inorganic clusters in its aqueous part.[18] In accordance with previous works dealing with a predictive approach to mesophase template structure formation,[14,18−20] the addition of surfactant was defined by the volume fraction of the surfactant after drying, Φ_{P123}, assuming that the inorganic phase is pure anatase ($\rho_{anatase} = 3.84$ g cm^{-3}) and the investigated range for Φ_{P123} was [0.5−0.75]. The selected value was $\Phi_{P123} = 0.68$. This value corresponds to the best quality and highest thermal stability of the ordered mesoporous structure in the prepared films, as previously observed for alumina layers.[18,20]

Sols that had been aged for 3 h, either without surfactant (samples T) or containing P_{123} (samples S), were used to prepare thin layers and equivalent powders. The thin layers were deposited by dip-coating (withdrawal rate = 10 cm min^{-1}) on flat soda−silica−lime glass slides and silicon wafers. Equivalent powders were obtained by pouring and drying the residual sols in large bakers. The high ratio between the volume of the sol and the surface of evaporation enabled us to obtain rapid drying and to minimize the effect of additional aging compared to the thin layers. The resulting cracked thick layers were ground to a powder. After being dried at room temperature for 24 h, the samples were thermally treated step by step up to 350 °C (step increase = 50 °C, dwell duration for each step = 2 h).The thermal elimination of the surfactant occurred in the range 150−250 °C (TGA analysis). In the case of thin layers of S that were thermally treated for 2 h at 150 °C, a UV irradiation treatment for 3 min provided for the complete elimination of the surfactant from the layer.

Characterization Methods. The mean hydrodynamic radius, R_H, of the titania colloids was determined from quasi-elastic light scattering (QLS) measurements. A micro-Raman spectrometer ($\lambda = 632.8$ nm, resolution = 2 cm^{-1}) was used for in situ structural characterization of the prepared sols, thin films, and powders. The crystalline structure of the oxide network and the ordering of the mesoporosity were investigated by X-ray diffraction (XRD) measurements performed with a diffractometer using a $\theta/2\theta$ Bragg−Brentano scattering geometry and Cu $L_{3,2}$ radiation. The crystallite size was estimated for the broadening of the diffraction peaks using the Scherrer relation.[21] UV spectra of powders dispersed in KBr pellets were recorded using a double-beam spectrometer (resolution = 2 nm). The porous texture of the powders was analyzed from nitrogen adsorption−desorption isotherms at 77 K. The BET and BJH methods[22] were applied for the determination of the specific surface area, S_{BET}, and the mean mesopore equivalent diameter, respectively. The porosity of a thin layer was investigated by coupling X-ray diffraction and nitrogen adsorption−desorption using an experimental device described in a previous paper.[23] Scanning electron microscopy (SEM) was performed to observe the morphology of the deposited layers.

The photocatalytic activity of the prepared layers was evaluated from an analysis of the photodegradation of stearic acid. The analytical method was derived from a previously described procedure.[24] A methanolic solution of stearic acid (0.02 mol·L^{-1}) was first deposited by dip-coating on one side of titania-coated or uncoated substrates. The immersion time and withdrawal rate were 1 min and 50 cm·min^{-1}, respectively. The substrates were then irradiated with a UV source (380 W m^{-2}, emission spectrum range of 200−450 nm, I_{max} at 384 nm). A Fourier transform infrared spectrometer was used to measure the evolution versus time of absorbance at 2850 cm^{-1}, corresponding to the maximum of the vibration band, ν_{C-H}, of stearic acid.

Results and Discussion

Stability and Structural Characteristics of the Titania Sols. The evolution of the colloid size as a function of the aging time after hydrolysis is shown in Figure 2. With the selected synthesis conditions, peptization of the initial precipitate occurred within 2 h. The resulting clear sol remained stable for 3 h. During this period of time, the mean hydrodynamic radius was kept roughly constant and equal to 6 nm. The aging temperature was found to be a very sensitive parameter. A small increase of a few degrees Celsius induced a decrease in the range of stability for the titania sol. For $\theta >$ 35 °C, no stability was observed.

(17) Chu, B.; Zhou, Z. In *Nonionic Surfactants: Polyoxyalkylene Block Copolymers*; Nace, V. M., Ed.; Marcel Dekker: New York, 1996; Vol. 60, p 67.
(18) Klotz, M.; Idrissi-Kandri, N.; Ayral, A.; Guizard, C. *Mater. Res. Soc. Symp. Proc.* **2000**, *628*, 7.4.1.
(19) Klotz, M.; Ayral, A.; Guizard, C.; Cot, L. *J. Mater. Chem.* **2000**, *10*, 663.
(20) Idrissi-Kandri, N.; Ayral, A.; Klotz, M.; Albouy, P. A.; El Mansouri, A.; van der Lee, A.; Guizard, C. *Mater. Lett.* **2001**, *50*, 57.
(21) Langford, J. I.; Wilson, A. J. C. *J. Appl. Cryst.* **1978**, *11*, 102.
(22) Lowell, S.; Shields, J. E. *Powder Surface Area and Porosity*; Chapman & Hall: London, 1984.
(23) Albouy, P.-A.; Ayral, A. *Chem. Mater.* **2002**, *14*, 3391.
(24) Ammerlaan, J. A. M.; McCurby, R. J.; Hurst, S. J. International Patent WO 00/75087 A1, 2000.

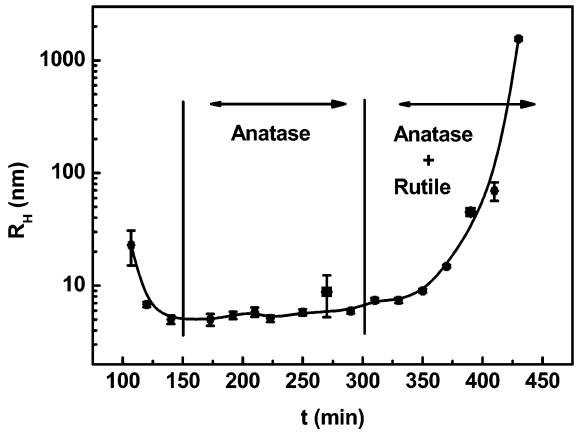

Figure 2. Evolution versus time of the mean hydrodynamic radius, R_H, of the colloidal titania particles.

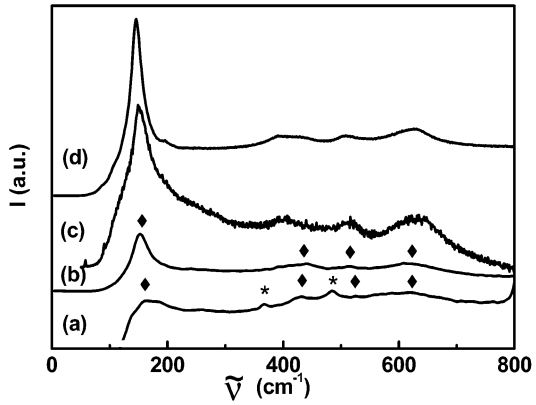

Figure 3. Raman spectra for (a) a sol aged for 3 h, (b) a powder obtained by drying the sol in a at 25 °C, (c) a thin layer of S thermally treated at 350 °C, and (d) a powder of S thermally treated at 350 °C (◆, anatase; *, 2-propanol).

The structure of the dispersed colloids was characterized in situ using Raman spectroscopy. The anatase and rutile forms of titania have been extensively studied by Raman spectroscopy; they present specific lines.[25−28] The Raman spectrum of the sol after 3 h of aging is shown in Figure 3a. This spectrum exhibits four bands located at 154, 430, 520, and 620 cm^{-1} that can be assigned to anatase. The formation of anatase is in agreement with the selected synthesis conditions: low temperature and low acid content (<2 M HCl).[29] Two additional bands located at 370 and 495 cm^{-1} can be assigned to 2-propanol,[30] which is produced by the titanium isopropoxide hydrolysis. The spectrum of the powder obtained by drying a titania sol at room temperature is reported in Figure 3b. The same bands related to anatase are observed, whereas the bands related to 2-propanol disappear after drying. The crystalline structure of the dried colloidal particles at room temperature is confirmed by XRD measurements. The corresponding pattern (Figure 4) shows broad and weak peaks with maxima in agreement with the positions reported for the most intense peaks of anatase in the

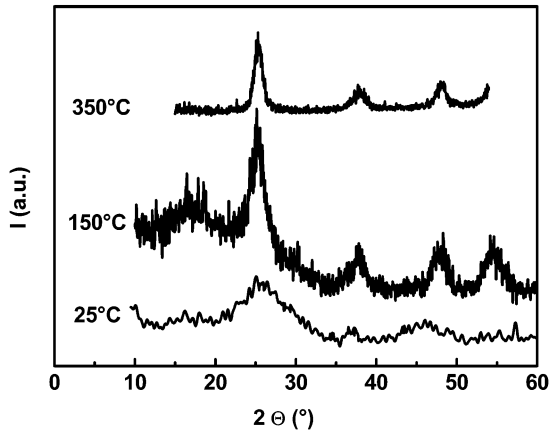

Figure 4. X-ray patterns for different powders of T: (a) dried at 25 °C, (b) thermally treated at 150 °C, and (c) thermally treated at 350 °C.

investigated angular range: I_{101}, I_{004}, I_{200}, and I_{211}.[31] An estimated crystallite size of about 5 nm was found from these broad peaks. It has been shown that hydrodynamic diameters measured for dispersed oxide colloids are always larger than the size of the associated solid particles,[32] so that it can be assumed that the nanoparticles of 12 nm in size detected by QLS correspond to the anatase nanocrystallites evidenced by XRD. It must be emphasized that the size of these crystallites allows their insertion into the aqueous domains of the mesophases formed with the triblock copolymer as the templating agent.[18] According to a comparison with powder diffraction standards,[31,33] the X-ray pattern of the precipitate obtained for aging times longer than 5 h corresponds to a mixture of anatase and rutile. The longer the aging time, the higher the rutile content. This phenomenon of dissolving and recrystallizing an oxide in its mother liquor to obtain a more stable crystalline phase has previously been reported for alumina.[34]

Textural and Structural Evolution with Temperature of the Titania Powders and Films. The structural evolution of the titania samples resulting from the drying of the sols was investigated by XRD and Raman spectroscopy. It must be noted that the Raman spectra (and also the later-described IR spectra) were recorded at room temperature. Consequently, the presence of adsorbed water hindered the study of the hydroxyl groups from these analyses. The XRD data show that the anatase/rutile transition occurs above 450 °C. A narrowing of the diffraction peaks is observed as the calcination temperature is increased (Figure 4). The associated evolution of the crystallite size is shown in Figure 5 for powders of T and S. Simultaneous with the increase of the crystallite sizes, there is a shift of the bands to lower frequencies in the Raman spectra. This phenomenon is particularly important for the main line initially centered on 150−154 cm^{-1}, which shifts to frequency values typically observed for well-crystallized anatase, 141−145 cm^{-1}. Although the broadening of this band cannot be directly correlated to the crystallite

(25) Melendres, C. A.; Narayanasamy, A.; Maroni, V. A.; Siegel, R. W. *J. Mater. Res.* **1989**, 4.
(26) Chang, H.; Huang, P. J. *J. Raman Spectrosc.* **1998**, *29*, 97.
(27) Parker, J. C.; Siegel, R. W. *Appl. Phys. Lett.* **1990**, *55*, 943.
(28) Parker, J. C.; Siegel, R. W. *J. Mater. Res.* **1990**, *5*, 1246.
(29) Jolivet, J. P. *De la Solution à l'Oxyde*; InterEditions/CNRS Editions: Paris, 1994.
(30) Venkateswarlu, K.; Mariam, S. *Z. Phy.* **1962**, *168*, 195.
(31) Joint Committee on Powder Diffraction Standards, Card No. 21-1276.
(32) Ayral, A.; Phalippou, J. *J. Eur. Ceram. Soc.* **1990**, *6*, 179.
(33) Joint Committee on Powder Diffraction Standards, Card No. 21-1272.
(34) Bye, G. C.; Robinson, J. G. *Kolloid Z. Z. Polym.* **1964**, *198*, 53.

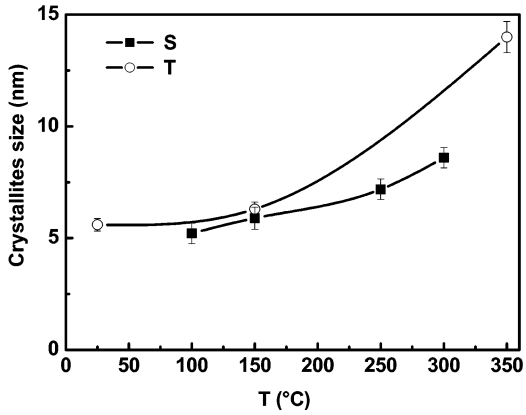

Figure 5. Evolution of the crystallite size versus temperature for powders of T and S.

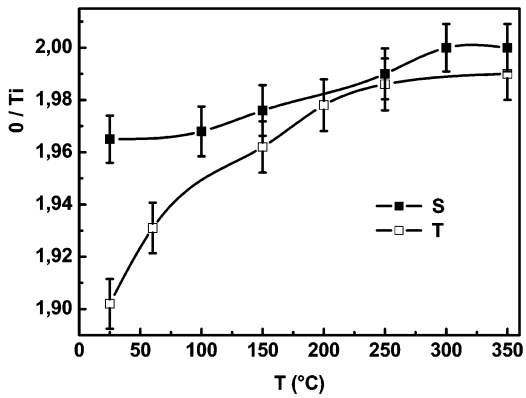

Figure 6. Evolution of the O/Ti ratio versus temperature for powders of T and S.

size,[25] its location is related to the oxygen deficiency of the oxide TiO_{2-x}.[27,28] Using the results of Parker and Siegel,[27,28] we calculated the O/Ti ratios associated with the location of the main Raman line of anatase. The resulting curves are presented in Figure 6, showing that the TiO_2 stoichiometry is obtained at 250−300 °C. A strong increase in absorbance between 400 and 350 nm is observed in the UV spectra of powders of T (Figure 7a). This absorbance increase shifts to slightly higher wavelengths as the temperature of the powder thermal treatment increases. This phenomenon is more clearly evidenced by the evolution of the position of the maximum in the derivative of the UV spectra, which corresponds to the inflection point on the spectrum (Figure 7b). It must be noted that the shape of the curve in Figure 7b is very close to that of the evolution of the O/Ti ratio for powders of T in Figure 6. The same comparison for powders of T is impeded by the presence of surfactant at low temperature, which disturbs the UV analyses.

Crack-free and homogeneous submicrometer-sized supported films were prepared from anatase sols of T and S (Figure 8). As the sol without surfactant was very fluid, the thickness of the layer after one dip-coating was very low (∼100 nm); thus, a second layer (∼200 nm) was deposited after thermal stabilization of the first one at 150 °C. The resulting bilayer structure appears in the image in Figure 8a. The thickness of a layer of S is about 400 nm (Figure 8b). Low-angle XRD patterns recorded for layers of S heat treated at different temperatures are shown in Figure 9. For a thermal treatment at 150 °C, without or with an additional UV

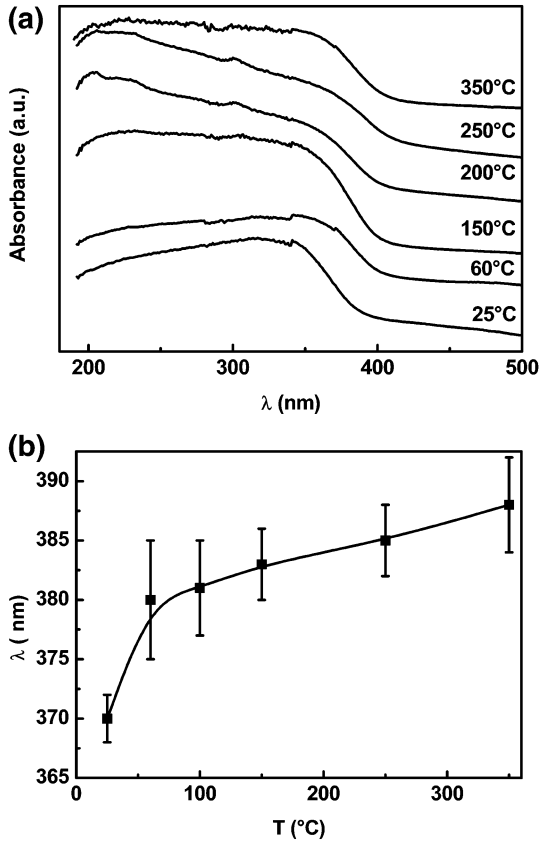

Figure 7. (a) UV spectra for a powder of T thermally treated at different temperatures. (b) Evolution of the position of the maximum in the derivative of the UV spectrum versus temperature.

treatment for complete elimination of the residual surfactant, the main diffraction peak observed corresponds to a Bragg *d* spacing equal to 88 nm, with a second weak peak at *d*/2. After the samples are heated at 350 °C, these peaks shift to higher diffraction angles. The Bragg spacing associated with the main diffraction peak is then equal to 56 nm. These results confirm the existence of an ordered mesostructure in the layers of S, but from the available data, it is not possible to determine the type of structure. The structure expected on the basis of the water−surfactant diagram is a bidimensional hexagonal structure consisting of close-packed cylindrical micelles. However, other structures that do not exist on the water−surfactant binary diagram could also be obtained.[35] Moreover, it has been shown that this kind of mesostructured layers can be strongly textured.[36] Additional investigations on the structure and texture of these layers are now required to determine the shape, the orientation, and a possible disortion of the mesopore network. 2D X-ray diffraction experiments and high-resolution transmission electron microscopy analyses are in progress to reach this goal.

Because of the difficulty in directly characterizing the porosity of supported thin films,[37] nitrogen adsorption−desorption measurements were carried out on the

(35) Besson, S. Ph.D. Thesis, Ecole Polytechnique, Paris, France, 2002.

(36) Klotz, M.; Albouy, P. A.; Ayral, A.; Menager, C.; Grosso, D.; van der Lee, A.; Cabuil, V.; Babonneau, F.; Guizard, C. *Chem. Mater.* **2000**, *12*, 1721.

(37) Ayral, A.; El Mansouri, A.; Vieira, M. P.; Pilon, C. *J. Mater. Sci. Lett.* **1998**, *17*, 883.

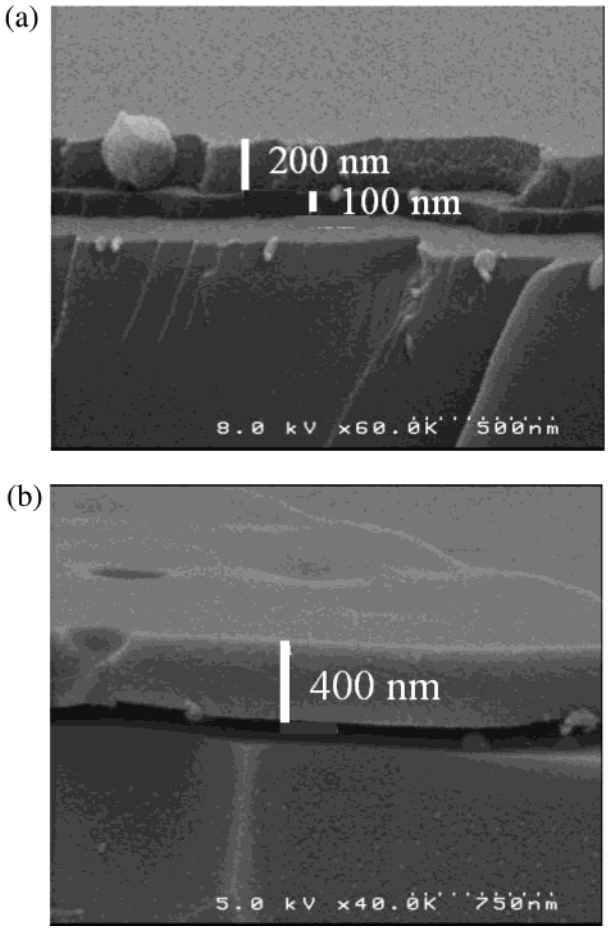

Figure 8. Cross-sectional SEM images of thin layers deposited on glass slides and thermally treated at 350 °C: (a) thin layer of T obtained after two successive dip-coatings and (b) thin layer of S.

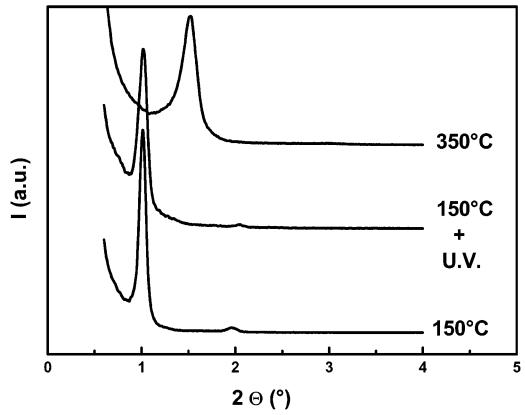

Figure 9. Low-angle X-ray patterns for a thin layer of S.

corresponding powders. In the case of a conventional sol−gel procedure, the final porosity is strongly dependent on the conditions of deposition, and differences are usually observed between supported thin layers and powders resulting from thick layers.[7] However, when the porosity is mainly generated by a templating effect, these differences are lower.[19] The isotherms obtained for powders of T and S are shown in Figure 10. These type IV isotherms are typical of mesoporous materials.[22] The main porous characteristics deduced from these isotherms are reported in Table 1. The porosity and S_{BET} of the powder obtained from a sol without surfactant (T) are very low compared to those of sample S. Powders

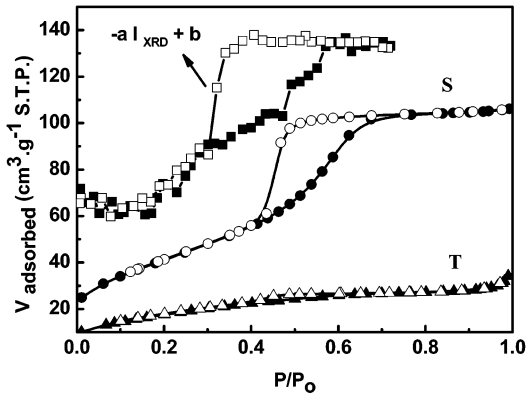

Figure 10. Nitrogen adsorption−desorption isotherms for powders of T and S thermally treated at 350 °C. The additional curve was established from the isothermal evolution of the intensity, I_{XRD}, of the main X-ray diffraction peak for a thin layer of S heated at 150 °C and then treated under UV irradiation for 3 min.

Table 1. Characteristics of the Porous Texture of Powders of T and S Heat Treated at 350 °C

	T	S
S_{BET} (m^2 g^{-1})	26	190
porosity (%)	8.5	39
mean BJH pore diameter determined from the adsorption branch (nm)	3.6	4.2

of S exhibit a sharp hysteresis loop related to a narrow pore size distribution. The mean equivalent BJH diameter determined from the adsorption branch is ∼4 nm, and the porosity is ∼40%. The high specific surface area, 190 m^2 g^{-1}, indicates that a significant fraction of the surface of the anatase nanocrystallites is accessible to nitrogen. Coupled X-ray diffraction and nitrogen adsorption measurements were performed on a layer of S treated at 150 °C with an additional UV treatment. A decrease of the diffracted intensity was observed with increasing nitrogen relative pressure. This phenomenon is due to additional X-ray absorption by the adsorbed gas and contrast variations in electron density.[23] The resulting isotherm exhibits a hysteresis loop associated with capillary condensation in the mesopores (Figure 10). The curve has been inverted to facilitate comparison with the other adsorption−desorption isotherms. The mean equivalent pore diameter estimated from the adsorption branch is around 3.5 nm.

Finally, assuming that the mesopores in layers of S treated at 350 °C are roughly equal to those measured in the powder, it appears that the pore size slightly increases and the mesoporous networks shrink during thermal treatment of layers of S from 150 to 350 °C.

Photocatalytic Activity of the Thin Layers. Several studies have focused on the photodegradation of organic compounds on titania layers. However, various experimental procedures have been applied that differ in the selected organic molecule, the medium, the emission spectrum, the power of the UV source, and the specific UV power measured on the surface of the titania layer. In this work, we adapted a procedure already described in the literature[24] that is based on an analysis of the degradation of stearic acid. Figure 11 shows the degradation curves for an uncoated silicon substrate, a substrate coated with a bilayer of type T, and a substrate coated with a monolayer of type S. No significant

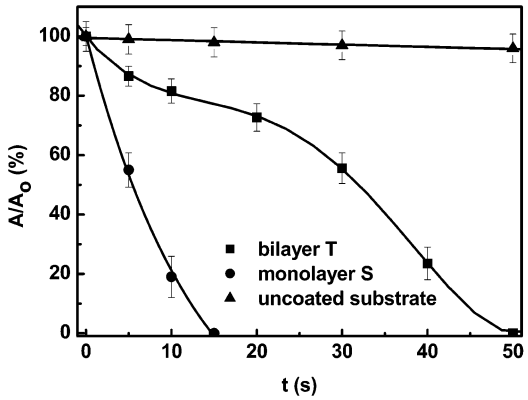

Figure 11. Evolution of the absorbance ratio A/A_0 as a function of UV irradiation time. A and A_0 are the absorbance values measured at 2850 cm^{-1} for the irradiated layer and for the initial layer, respectively.

degradation is observed for the uncoated substrate after 50 s of UV irradiation, whereas degradation is complete after 15 and 50 s for the layers of S and T, respectively. The decrease in the amount of stearic acid for the bilayer of T occurs in two successive stages (Figure 11). This phenomenon could be related to a difference in the porous texture between the two successive layers. The amount of stearic acid deposited per unit area is expected to be more important with respect to layers of S, assuming that this value increases with both layer thickness and specific surface area of the deposited solid. However, this layer is the most efficient in terms of degradation kinetics. Its higher efficiency can be explained by its higher porosity, which favors the transport of oxygen inside the layer and the extraction of the degradation products. The specific power of the UV device used , 380 W m^{-2}, is ∼12 times larger than that used in ref 24, 32 W m^{-2}. Unfortunately, no reference titania layer is currently available, unlike the case for the powders with commercial products such as Degussa P25. To compare the performance of our layers with those described in ref 24, the times of irradiation for 90% degradation were multiplied by a factor 12 to estimate an equivalent time in terms of UV energy received by the titania surface. In the case of layers of S, the corresponding value, 2 min, is shorter than that obtained for the layers tested in ref 24 ($4 < t_{90\%} < 15$ min). Additional qualitative evidence of the photocatalytic efficiency of layers of S is given by the experiment on UV degradation of the residual surfactant for a layer previously treated for 2 h at 150 °C. Figure 12 shows the evolution of the IR spectrum in the frequency range 3100−2700 cm^{-1} and the progressive disappearance of the ν_{C-H} vibration bands of the surfactant. In any case, it can also be noted that no absorption band associated with the presence of carboxylate groups possibly generated by the photodegration of the organic compounds was evidenced in the IR spectra.

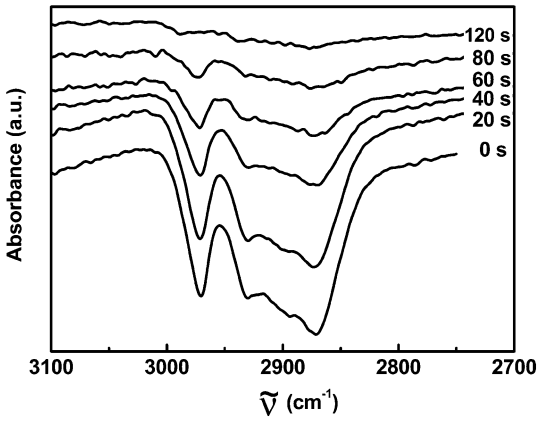

Figure 12. IR spectra of a thin layer of S thermally treated at 150 °C and irradiated for different times.

Conclusions

A simple sol−gel method has been developed for the preparation of mesoporous and nanocrystalline titania thin layers from titanium isopropoxide. The optimization of the synthesis parameters enabled the room-temperature preparation of clear sols consisting of dispersed anatase nanocrystallites. Supported thin layers and corresponding powders were prepared from these sols. By the addition of a templating agent to the starting sols, the porosity and specific surface area were improved, and layers exhibiting ordered mesoporosity were prepared. It was observed that the rutile form appears only above 450 °C. The thermal evolution of the crystallite size, of the stoichiometry, and of the UV spectrum of the anatase phase was studied. The results suggest a strong relationship between crystallite size and O/Ti stoichiometry on one hand and the preparation method on the other. Preliminary experiments on the photocatalytic efficiency of the anatase thin layers support the mesostructured layers. Interestingly, it is possible to completely eliminate the templating agent by the UV irradiation of a thin layer previously heated at 150 °C. The preparation of mesoporous and nanocrystalline anatase layer on substrates with low thermal stability can be thus considered.

This paper describes results on thin films deposited on dense substrates, but layers have also been successfully deposited on porous substrates. Future work directed toward coupling membrane separation and photocatalyic reaction is now scheduled using ceramic membranes with such anatase top layers.

Acknowledgment. The authors thank D. Cot, N. Kourda, A. El Mansouri, E. Petit, and A. van der Lee (IEM) for their help with the characterization of the samples.

CM031025A